HHS Public Access

Author manuscript

Dev Biol. Author manuscript; available in PMC 2016 April 01.

Published in final edited form as:

Dev Biol. 2015 April 1; 400(1): 82–93. doi:10.1016/j.ydbio.2015.01.018.

Fibroblast growth factor receptor–Frs2α signaling is critical for nephron progenitors

Valeria Di Giovanni[a], **Kenneth A. Walker**[a], **Daniel Bushnell**[a], **Caitlin Schaefer**[a], **Sunder Sims-Lucas**[a], **Pawan Puri**[a], and **Carlton M. Bates**[a,b,*]

[a]Division of Nephrology, Department of Pediatrics, University of Pittsburgh School of Medicine, Pittsburgh, PA 15201, USA

[b]Rangos Research Center, Children's Hospital of Pittsburgh of UPMC, Pittsburgh, PA 15224, USA

Abstract

Previous studies using transgenic Pax3cre mice have revealed roles for fibroblast growth factor receptors (Fgfrs) and Fgfr substrate 2α (Frs2α) signaling in early metanephric mesenchyme patterning and in ureteric morphogenesis. The role of Fgfr/Frs2α signaling in nephron progenitors is unknown. Thus, we generated mouse models using BAC transgenic *Six2EGFP*cre (Six2cre) mediated deletion of Fgfrs and/or Frs2α in nephron progenitors. *Six2cre* mediated deletion of *Fgfr1* or *Fgfr2* alone led to no obvious kidney defects. *Six2creFgfr1*$^{flox/flox}$*Fgfr2*$^{flox/flox}$ (*Fgfr1/2*$^{NP-/-}$) mice generate a discernable kidney; however, they develop nephron progenitor depletion starting at embryonic day 12.5 (E12.5) and later demonstrate severe cystic dysplasia. To determine the role of Frs2α signaling downstream of Fgfr2 in *Fgfr1/2*$^{NP-/-}$ mice, we generated *Six2cre·Fgfr1*$^{flox/flox}$*Fgfr2*$^{LR/LR}$ (*Fgfr1*$^{NP-/-}$*Fgfr2*$^{LR/LR}$) mice that have point mutations in the Frs2α binding site of Fgfr2. Like *Fgfr1/2*$^{NP-/-}$ mice, *Fgfr1*$^{NP-/-}$*Fgfr2*$^{LR/LR}$ develop nephron progenitor depletion, but it does not start until E14.5 and older mice have less severe cystic dysplasia than *Fgfr1/2*$^{NP-/-}$ To determine the role of Frs2α alone in nephron progenitors, we generated *Six2creFrs2′A*$^{flox/flox}$ (*Frs2a*$^{NP-/-}$) mice. *Frs2a*$^{NP-/-}$ mice also develop nephron progenitor depletion and renal cysts, although these occurred later and were less severe than in the other Six2cre mutant mice. The nephron progenitor loss in all *Six2cre* mutant lines was associated with decreased Cited1 expression and increased apoptosis versus controls. FAC-sorted nephron progenitors in *Six2cre Frs2′A*$^{flox/flox}$ mice demonstrated evidence of increased Notch activity versus controls, which likely drives the progenitor defects. Thus, Fgfr1 and Fgfr2 have synergistic roles in maintaining nephron progenitors; furthermore, Fgfr signaling in nephron progenitors appears to be mediated predominantly by Frs2α.

*Corresponding author at: Rangos Research Center, Children's Hospital of Pittsburgh of UPMC, Pittsburgh, PA 15224, USA. Fax: +1 412 692 7756. batescm@upmc.edu (C.M. Bates).

Statement of competing financial interests

The authors have no financial interests to report.

Keywords

Fibroblast growth factor receptors; Frs2α; Nephron progenitors; Kidney development

Introduction

Mammalian kidney development occurs via reciprocal interactions between the metanephric mesenchyme and ureteric epithelium (Little and McMahon, 2012). Signaling from the metanephric mesenchyme (MM) induces formation of the ureteric bud (UB) from the nephric duct, which elongates and branches to ultimately form the renal collecting ducts, pelvis, and ureter. Simultaneously, nephron progenitors, a subpopulation of MM cells, form a cap mesenchyme (CM) around UB tips that either self-renew or differentiate into nephrogenic epithelia (which progress from renal vesicles to comma-shaped bodies, S-shaped bodies and finally immature glomeruli). The other mesenchymal lineage, the cortical renal stroma, surrounds and interacts with nephron progenitors and the ureteric epithelium.

Previous work has demonstrated essential roles for fibroblast growth factor receptor signaling during kidney formation (Perantoni et al., 1995, 2005; Barasch et al., 1997; Celli et al., 1998; Zhao et al., 2004; Grieshammer et al., 2005; Poladia et al., 2006; Hains et al., 2008, 2010; Sims-Lucas et al., 2009a, 2011a, 2011b, 2012; Walker et al., 2013). Fgfr proteins are receptor tyrosine kinases, which signal using intracellular adapter molecules. Frs2α, a major adapter molecule constitutively bound to Fgfr juxtamembrane domains, becomes phosphorylated upon receptor stimulation leading to activation of Erk, Akt, and alternative forms of protein kinase C (Ong et al., 2000; Powers et al., 2000). While global deletion of *Fgfr3* or *Fgfr4* does not affect kidney morphogenesis in mice (Colvin et al., 1996; Weinstein et al., 1998), loss of *Fgfr1*, *Fgfr2*, or *Frs2α* leads to early embryonic lethality prior to kidney formation (Deng et al., 1994; Yamaguchi et al., 1994; Arman et al., 1998; Xu et al., 1998; Gotoh et al., 2005).

Our laboratory has utilized conditional knockout, receptor isoform knockout, and receptor point mutation mouse models to elucidate the roles of Fgfr and Frs2α signaling in the developing kidney (Zhao et al., 2004; Poladia et al., 2006; Hains et al., 2008, 2010; Sims-Lucas et al., 2009a, 2011a, 2011b, 2012; Walker et al., 2013). Previously, we found that *Pax3*cre mediated deletion of *Fgfr1* and *Fgfr2* in early metanephric mesenchyme ($Fgfr1/2^{MM-/-}$) together resulted in severe renal dysgenesis, demonstrating the critical and redundant roles of these receptors in establishing early kidney mesenchyme (Poladia et al., 2006). The severity of the renal defects in these mice precluded the ability to determine the role of Fgfr signaling in the nephron progenitor lineage. In a separate study, we found that mice with *Pax3*cre deletion of *Fgfr1* and with point mutations in the *Frs2α* binding site of *Fgfr2* (Leucine 424 and Arginine 426, called the “LR” allele) ($Fgfr1^{MM-/-}Fgfr2^{LR/LR}$) developed dilated UB tips and cystic kidneys; however, the early Six2 marked nephron progenitor population appeared normal (Sims-Lucas et al., 2012).

Given that the *Pax3cre* transgenic line drives cre expression early in both renal stromal and nephrogenic mesenchyme, we sought to determine the specific cell autonomous requirement for Fgfr and/or Frs2α signaling in the nephrogenic lineage (nephron progenitors and/or their

downstream derivatives). Thus, we generated a *Six2-EGFPcre*-driven allelic series of mice that remove *Fgfr* and/or *Frs2α* expression in the more restricted nephron progenitor population and at a slightly later embryonic age than the *Pax3cre* mutants (Li et al., 2000; Kobayashi et al., 2008). The first were *Six2cre Fgfr1*$^{flox/flox}$*Fgfr2*$^{flox/flox}$ mice, which delete *Fgfr1* and *Fgfr2* expression in nephron progenitors. Next, we generated *Six2cre, Fgfr1*$^{flox/flox}$*Fgfr2*$^{LR/LR}$ mice which delete *Fgfr1* in nephron progenitors and carry the "LR" Fgfr2 point mutation that blocks Frs2α binding. Finally we generated *Six2cre Frs2′A*$^{flox/flox}$ mice, which delete Frs2α expression in nephron progenitors (but which would allow Fgfr1 and Fgfr2 signaling through alternative adapters). We compared these mice to one another and to the previously described *Pax3cre* mutants to elucidate a novel role for Fgfr/Frs2α signaling in the nephron progenitor population.

Materials and methods

Experimental mouse models

Transgenic *Six2-EGFPcre* (*Six2-EGFPcre*) mice (Kobayashi et al., 2008) and/or transgenic *Pax3cre* mice (gift from Jon Epstein) (Li et al., 2000), which express cre in nephron progenitors and global metanephric mesenchyme, respectively, were bred with *Fgfr1*$^{flox/flox}$ mice (gift from Janet Rossant) (Hebert et al., 2003), *Fgfr2*$^{flox/flox}$ mice (gift from David Ornitz) (Ornitz and Marie, 2002), Frs2α$^{flox/flox}$ mice (gift from Fen Wang) (Lin et al., 2007), and/or *Fgfr2*$^{LR/LR}$ mice, which have Fgfr2 point mutations converting amino acids Leu-424 (L) and Arg-426 (R) to Ala residues to prevent Frs2α association with Fgfr2 (gift from VP Eswarakumar) (Eswarakumar et al., 2006; Sims-Lucas et al., 2009b). The presence of a copulatory plug in the morning was considered E0.5. Genotyping was performed by PCR, using genomic DNA isolated from tail clippings or embryonic tissue. All animals were housed in the vivarium at the Rangos Research Center, at the Children's Hospital of the University of Pittsburgh. All experiments were approved by the University of Pittsburgh Institutional Animal Care and Use Committee.

Tissue collection, qPCR and FAC-sorting

Histological experiments were performed by fixing embryos or kidneys in 4% paraformaldehyde (PFA) at 4 °C overnight and embedding in paraffin blocks. Tissue sections were then subjected to hematoxylin and eosin (H&E) staining, immunostaining, or in situ hybridization (ISH). Section in situ hybridization was performed on tissue sections (8 μm) as described (Di Giovanni et al., 2011). Digoxigenin labeled antisense and sense RNA probes were created for *Bmp7*, *Eya1*, *Lhx1*, *Wnt4*, *Osr1*, *Fgfr1*, and *Fgfr2* as described (Di Giovanni et al., 2011).

For FAC-sorting, GFP expression was utilized to sort nephron progenitors from E14.5 *Six2-EGFPcreFrs2α* $^{flox/flox}$ (*Frs2a*$^{NP-/-}$) and *Six2-EGFPcreFrs2α* $^{flox/+}$ (heterozygous control) animals. Kidneys were collected from animals with the previously described genotypes and were digested in a 0.3% collagenase solution (Gibco, NY) for 10 min at 37 °C, followed by several rapid passages through a 25-gauge syringe to produce a single cell suspension. Cells were washed several times in a 10% FBS solution. GFP-positive nephron progenitor cells were collected in RNAeasy (Qiagen, CA) and stored at −80 °C for RNA extraction.

Approximately 50,000 cells of the same genotype were pooled from 3–4 litters (*n*=6 pools of cells per genotype).

RNA was extracted from snap frozen E13.5 *Fgfr1*$^{NP-/-}$*Fgfr2*$^{LR/LR}$ and cre negative control kidneys (*n*=3 per genotype, 4 kidneys per group) or FAC-sorted GFP-positive E14.5 *Frs2a*$^{NP-/-}$ and heterozygous control cells. RNA extraction was performed using the RNAeasy Plus MicroKit (Qiagen, GmbH). Using the Beacon Designer software program, primers for *Bmp7*, *Brpf1*, *Cited1*, *Ctnnb1*, *Dpf3*, *Eya1*, *HeyL*, *Jagged1*, *Meox1*, *Notch1*, *Osr1*, *Six2* and *Wnt9b* and the endogenous control *Gapdh* were designed and manufactured (Invitrogen, CA). The Superscript First Strand cDNA kit (Invitrogen, CA) and a C1000 Thermal Cycler (Biorad, CA) were used to perform the qPCR assays.

3-Dimensional (3D) reconstruction

3D reconstructions of E13.5 control and *Fgfr1*$^{NP-/-}$*Fgfr2*$^{LR/LR}$ kidney capsules, developing nephrons, ureteric trees and ureters were performed as described (Sims-Lucas et al., 2009a). Briefly, image layers were created from projected serial H&E stained sections (4 μm) by tracing around capsules, nephrogenic structures (vesicles, comma-shaped bodies, S-shaped bodies, and immature glomeruli), and the ureteric tree (Stereoinvestigator, Microbrightfield, MBF, and VT). Traced layers were aligned and rendered into a 3D graphical reconstruction, from which ureteric tip number and ureteric volumes were determined.

Immunofluorescence and whole mount immuno*fl*uorescence experiments

Immunofluorescent microscopy was performed using 8 μm paraffin sections washed in xylene and re-hydrated in ethanol. Sections were heated in a pressure cooker in 0.1 M sodium citrate buffer (pH 6.0), blocked in a 30% BSA/donkey serum solution, and incubated with primary antibodies overnight at 4 °C. Tissue was incubated with either Alexa Fluor 488/594 goat-anti-mouse or anti-rabbit secondary antibodies (1:500, Invitrogen) and DAPI for 1 h at room temperature, mounted in VectaShield (Vector Labs, CA), and visualized on a Leica DM2500 fluorescent microscope. The primary antibodies that were utilized were: anti-Cited1 (1:200, NeoMarkers, MI), anti-Jagged1 (1:100, Santa Cruz, TX) anti- Notch1 (1:100, Cell Signaling, MA), anti-NCAM (1:200, Sigma, MO), anti-Six2 (1:200, Proteintech, IL), and anti-Frs2α 1: 1:100 (Abcam, MA). DBA and LTL lectins were used at a dilution of 1:200 (Vector Labs, CA).

Apoptosis and cell proliferation assays

Terminal deoxynucleotidyl transferase dUTP nick-end labeling (TUNEL) assays on *Fgfr1/2*$^{NP-/-}$, *Fgfr1*$^{NP-/-}$*Fgfr2*$^{LR/LR}$, *Frs2a*$^{NP-/-}$, and control tissue sections (*n*=3 per genotype) were performed using an ApopTag Plus Fluorescein In Situ Apoptosis Detection kit (Millipore, CA) on paraffin sections (8 μm) following the manufacturer's instructions. For the TUNEL assays, cortical kidney area was determined by measuring the outline of the developing nephrogenic zone on sagittal sections taken through the kidney midline using Image J software (NIH, MD); apoptosis was quantitated as a percentage of positive cells per nephrogenic zone. To examine cell proliferation, antigen retrieval was performed as outlined previously and tissue was incubated with anti-NCAM (1:200, Sigma, MO) and anti-phosphohistone H3 (1:200, Sigma, MO) overnight at 4 °C. Cells that stained with both

phosphohistone H3 (proliferating) and NCAM (nephrogenic compartment) were counted and compared in controls versus *Fgfr1*$^{NP-/-}$*Fgfr2*$^{LR/LR}$ animals (n=3 per genotype, 2 sections per animal).

Statistical analyses

Statistical analyses of developing nephron structure number, the rate of apoptosis and qPCR experiments were performed on biological replicates using a Student's *t*-test (Excel). All values are represented as means±standard error with $p<0.05$ considered significant.

Results

Fgfr1/2 signaling is crucial for maintenance of the nephron progenitor population

To determine whether Fgfr signaling was required in nephron progenitors, we used *Six2creFgfr1*$^{flox/flox}$*Fgfr2*$^{flox/flox}$ mice to delete Fgfr1 and/or Fgfr2 in this population. We confirmed relatively efficient transgenic *Six2cre* driven deletion of *Fgfr1* and *Fgfr2* in nephron progenitors by in situ hybridization (Fig. 1). Despite this, we noted no defects in mice with *Six2cre* driven loss of *Fgfr1* or *Fgfr2* alone (and even with three out of four alleles deleted) (not shown). Furthermore, unlike *Pax3creFgfr1*$^{flox/flox}$*Fgfr2*$^{flox/flox}$ mice that formed no discernable kidneys, (Poladia et al., 2006), E12.5 *Fgfr1/2*$^{NP-/-}$ kidneys appeared relatively normal and expressed the mesenchymal genes Six2, *Osr1*, *Bmp7* and *Lhx1* (Figs. 2 and S1). By E13.5, however, *Fgfr1/2*$^{NP-/-}$ mutants demonstrated depletion of Six2 marked nephron progenitors (Fig. 2). Moreover, E12.5 *Fgfr1/2*$^{NP-/-}$ nephron progenitors showed excessive apoptosis by fluorescent TUNEL staining versus controls (control: 33±13%, mutant: 73±5%, $^{*}p<0.01$) (Fig. 2). In addition, E13.5 *Fgfr1/2*$^{NP-/-}$ nephron progenitors expressed virtually no Cited1, a marker of the un-induced self-renewing nephron progenitor sub-compartment (Boyle et al., 2008) (Fig. 2). By E18.5, *Fgfr1/2*$^{NP-/-}$ mutants had small, cystic dysplastic kidneys with an underdeveloped Six2-positive nephrogenic zone, a reduced number of developing nephron structures, and dilated tubules (Fig. 2). *Fgfr1/2*$^{NP-/-}$ mice were not viable after birth. Thus, deletion of both *Fgfr1* and *Fgfr2* in nephron progenitors resulted in loss of progenitors by apoptosis, loss of Cited1 expression, and renal cystic dysplasia.

Loss of Fgfr–Frs2α signaling in nephron progenitors also results in autonomous defects

To begin to interrogate the contribution of Frs2α-mediated Fgfr signaling in nephron progenitors, we then examined *Six2cre Fgfr1*$^{flox/flox}$*Fgfr2*$^{LR/LR}$ (*Fgfr1*$^{NP-/-}$*Fgfr2*$^{LR/LR}$) mice, which delete *Fgfr1* in nephron progenitors (Fig. 1) and that have point mutations in the Frs2α binding site on Fgfr2. Unlike *Fgfr1/2*$^{NP-/-}$ mice, E13.5 *Fgfr1*$^{NP-/-}$*Fgfr2*$^{LR/LR}$ nephron progenitors appeared relatively normal by Six2 immunofluorescence and H&E staining (Figs. 3 and 5); however, by E14.5 and persisting through E18.5, a substantial number of *Fgfr1*$^{NP-/-}$*Fgfr2*$^{LR/LR}$ nephron progenitors appeared to be depleted by Six2 staining relative to controls (Fig. 3). TUNEL staining demonstrated a dramatic increase in the number of apoptotic cells in the cortical mesenchyme of E13.5 *Fgfr1*$^{NP-/-}$*Fgfr2*$^{LR/LR}$ kidneys versus controls (controls: 6±2%; *Fgfr1*$^{NP-/-}$*Fgfr2*$^{LR/LR}$: 42±7%, $^{*}p<0.01$) (Fig. 3), while E13.5 mutant and control nephron progenitor proliferation rates appeared equivalent by phosphohistone H3 staining (Fig. S2). Thus, the *Fgfr1*$^{NP-/-}$*Fgfr2*$^{LR/LR}$ increases in

apoptosis and reduction in nephron progenitors occurred slightly later than in *Fgfr1/2*$^{NP-/-}$ mice.

By E18.5, *Fgfr1*$^{NP-/-}$*Fgfr2*$^{LR/LR}$ embryonic kidneys displayed tubular dilatation/cysts derived from nephron lineages including glomeruli and proximal tubules, while ureteric bud-derived collecting ducts appeared normal (Fig. 4). Unlike *Fgfr1/2*$^{NP-/-}$ mice, a small percentage of *Fgfr1*$^{NP-/-}$*Fgfr2*$^{LR/LR}$ pups survived after birth. In surviving *Fgfr1*$^{NP-/-}$*Fgfr2*$^{LR/LR}$ mutants, the tubular dilation was progressive and resulted in almost complete replacement of the renal parenchyma by cysts at post-natal day 21 (Fig. 4). Thus, while the cystic disease in *Fgfr1*$^{NP-/-}$*Fgfr2*$^{LR/LR}$ kidneys appeared to progress more slowly than in *Fgfr1/2*$^{NP-/-}$ mice, ultimately, *Fgfr1*$^{NP-/-}$*Fgfr2*$^{LR/LR}$ mutants ended up with severe cystic changes.

We then compared *Fgfr1*$^{NP-/-}$*Fgfr2*$^{LR/LR}$ mice with *Pax3-creFgfr1*$^{flox/flox}$*Fgfr2*$^{LR/LR}$ (*Fgfr1*$^{MM-/-}$*Fgfr2*$^{LR/LR}$) mice in which Fgfr1 is deleted throughout the entire metanephric mesenchyme. While we previously found that E13.5 *Fgfr1*$^{MM-/-}$*Fgfr2*$^{LR/LR}$ mice had dilated and fewer ureteric tips (Sims-Lucas et al., 2012), E13.5 *Fgfr1*$^{NP-/-}$*Fgfr2*$^{LR/LR}$ ureteric tips appeared normal by H&E staining and showed no changes in average ureteric epithelium volume or tip number by 3D reconstruction versus controls (control volume: $28.7 \times 10^4 \pm 4.03 \times 10^4$ μm^3, *Fgfr1*$^{NP-/-}$*Fgfr2*$^{LR/LR}$: $27.6 \times 10^4 \pm 2.20 \times 10^4$ μm^3, p=0.81) (control tips: 75±18, *Fgfr1*$^{NP-/-}$*Fgfr2*$^{LR/LR}$: 46±11, p=0.16) (Fig. 4). We also found that unlike E18.5 *Fgfr1*$^{NP-/-}$*Fgfr2*$^{LR/LR}$ mice that had no collecting duct dilatation (see Fig. 4), E18.5 *Fgfr1*$^{MM-/-}$*Fgfr2*$^{LR/LR}$ embryos did develop dilated tubules from both nephron and ureteric lineages (Fig. S3). We then assessed whether *Fgfr1*$^{MM-/-}$*Fgfr2*$^{LR/LR}$ mice had previously unrecognized nephron progenitor depletion. Indeed, Six2 staining revealed loss in the *Fgfr1*$^{MM-/-}$*Fgfr2*$^{LR/LR}$ nephron progenitor population at E18.5 compared with controls (Fig. S4). Thus, the *Fgfr1*$^{MM-/-}$*Fgfr2*$^{LR/LR}$ and *Fgfr1*$^{NP-/-}$*Fgfr2*$^{LR/LR}$ lines expose temporal and/or spatial windows of Fgfr/Frs2α activity in kidney mesenchyme in repressing cystogenesis in different renal lineages. However, the *Fgfr1*$^{NP-/-}$*Fgfr2*$^{LR/LR}$ and *Fgfr1*$^{MM-/-}$*Fgfr2*$^{LR/LR}$ mice also reveal that Fgfr/Frs2α signaling in the nephron progenitor compartment is critical for nephron progenitor survival.

We then sought to determine if there were intrinsic defects in the *Fgfr1*$^{NP-/-}$*Fgfr2*$^{LR/LR}$ mutant nephron progenitor population. At E13.5, *Fgfr1*$^{NP-/-}$*Fgfr2*$^{LR/LR}$ and control kidneys had comparable expression of the renal mesenchyme markers *Eya1*, *Osr1*, *Meox1*, *Brpf1* and *Dpf3* (Mugford et al., 2009) (Fig. 6). In addition, expression of Cited1 was decreased in E13.5 *Fgfr1*$^{NP-/-}$*Fgfr2*$^{LR/LR}$ kidneys by both qPCR and by immunostaining (Fig. 6), similar to *Fgfr1/2*$^{NP-/-}$ kidneys. Six2mRNA levels appeared to be trending down in E13.5 mutants versus controls. Thus, while many markers were expressed normally in E13.5 *Fgfr1*$^{NP-/-}$*Fgfr2*$^{LR/LR}$ nephron progenitors, there was a trend for decreased Six2 mRNA expression and a marked reduction of Cited1 mRNA and protein. Thus, *Fgfr1*$^{NP-/-}$*Fgfr2*$^{LR/LR}$ nephron progenitors were depleted, similar to what was seen in *Fgfr1/2*$^{NP-/-}$ kidneys, albeit with a delayed onset.

Given that the changes in *Fgfr1*$^{NP-/-}$*Fgfr2*$^{LR/LR}$ nephron progenitors (increased apoptosis and loss of Cited1) started at E13.5, we examined E13.5 *Fgfr1*$^{NP-/-}$*Fgfr2*$^{LR/LR}$ mice for

alterations in factors known to regulate nephron progenitors, by tissue staining and qPCR on whole kidney mRNA. Examination of *Bmp7*, a growth factor linked to nephron progenitor survival (Blank et al., 2009), by qPCR and in situ hybridization, revealed no significant difference in expression in E13.5 $Fgfr1^{NP-/-}Fgfr2^{LR/LR}$ kidneys or nephron progenitors compared to controls (Fig. 7). Second, immunostaining and/or qPCR on whole kidney mRNA revealed no changes in $Fgfr1^{NP-/-}Fgfr2^{LR/LR}$ kidney expression of *Wnt9b* or canonical Wnt readouts β-catenin and *Lef1* (Fig. 7), all components of a pathway that directs nephron progenitor cells to exit the self-renewing stem cell niche (Karner et al., 2011). Finally, immunostaining for p53, recently identified as critical for nephron progenitor survival (Saifudeen et al., 2012), was unaltered in $Fgfr1^{NP-/-}Fgfr2^{LR/LR}$ kidneys (Fig. 7). Thus it appears that Bmp7, Wnt9b, and p53 signaling (all of which are known to be important for nephron progenitor survival) is intact in $Fgfr1^{NP-/-}Fgfr2^{LR/LR}$ mice.

Loss of Frs2α expression in nephron progenitors also leads to autonomous defects

To fully elucidate the importance of Frs2α-mediated Fgfr signaling in nephron progenitors, we compared $Fgfr1/2^{NP-/-}$ and $Fgfr1^{NP-/-}Fgfr2^{LR/LR}$ mice to $Six2creFrs2\alpha^{flox/flox}$ ($Frs2a^{NP-/-}$) mice, which lose Frs2α expression in nephron progenitors. Like the other mutants, $Frs2a^{NP-/-}$ mice demonstrated a decrease in Six2-labeled nephron progenitors, but not until E15.5 (Fig. 8), later than both $Fgfr1/2^{NP-/-}$ and $Fgfr1^{NP-/-}Fgfr2^{LR/LR}$ mice. Moreover, $Frs2a^{NP-/-}$ nephron progenitors had a loss of Cited1 expression (Fig. 8) and excessive nephron progenitor apoptosis versus controls (control: 1±1%, mutant: 6±2%, $p<0.05$) (Fig. 8), but again slightly later at E14.5. By E18.5, $Frs2a^{NP-/-}$ mice displayed tubular dilatation/cysts and smaller kidneys than controls (Fig. 8), albeit less severe than E18.5 $Fgfr1/2^{NP-/-}$ or $Fgfr1^{NP-/-}Fgfr2^{LR/LR}$ mice. While most $Frs2a^{NP-/-}$ mice survived after birth, after a week cysts were easily detected in mutant mice and by P30, $Frs2a^{NP-/-}$ mutant kidneys had severe cystic dysplasia, similar to P21 $Fgfr1^{NP-/-}Fgfr2^{LR/LR}$ mice (Fig. S5).

Given that the nephron progenitor defects in $Frs2a^{NP-/-}$ mice occurred later than in $Fgfr1/2^{NP-/-}$ and $Fgfr1^{NP-/-}Fgfr2^{LR/LR}$ mutants, we were able to use FAC-sorting to isolate and pool sufficient numbers of E14.5 $Frs2a^{NP-/-}$ nephron progenitors for qPCR assessment of other candidate pathways disrupted downstream of the *Six2cre* mutants. First, we confirmed decreased *Frs2α* and *Cited1* mRNA from pooled mutant nephron progenitors versus controls (Fig. 9). We also found equivalent *Six2* and *Bmp7* mRNA levels in E14.5 $Frs2a^{NP-/-}$ pooled progenitors versus controls (Fig. 9). We also detected marginal (~12%) increases in p53 mRNA in mutant progenitors compared with controls (as opposed to decreases, which might be expected with nephron progenitor loss). While Egf and Tgfα appear to support nephron progenitor survival in vitro (Brown et al., 2011), *Egf* mRNA was unchanged and *Tgfα* mRNA was only marginally decreased in E14.5 $Frs2a^{NP-/-}$ mutant cells versus controls by qPCR (Fig. S6). In contrast, Notch signaling, a pathway known to be critical in driving nephron differentiation (Cheng et al., 2007), appeared altered in $Frs2a^{NP-/-}$ mutant cells. qPCR revealed significant increases in *Notch1* and *HeyL* (Notch signaling readout) and a trend for increased *Jagged1* (Notch ligand) in groups of pooled $Frs2a^{NP-/-}$ nephron progenitor cells versus controls (Fig. 9). Immunostaining for Notch1 and Jagged1 appeared to show increased protein expression in nephron progenitors (and

possibly in nephron derivatives). Thus, Notch signaling appears increased in isolated *Frs2a*$^{NP-/-}$ nephron progenitors compared to controls.

Discussion

Much of the previous work on Fgf signaling in nephron progenitors has focused on Fgf ligands. Conditional inactivation of *Fgf8* in metanephric mesenchyme cells (stroma and nephron progenitors) led to nephron progenitor depletion and a block in nephron development after the renal vesicle stage (Grieshammer et al., 2005; Perantoni et al., 2005). Our data strongly suggests that Fgf8 is likely not the direct ligand for Fgfr1 or 2 in nephron progenitors, given that none of our *Fgfr/Frs2α* mutants have a block in nephrogenesis and that the onset of nephron progenitor apoptosis was later in *Fgf8* mutants than in *Fgfr1/2*$^{NP-/-}$ mice. Also, more recent work showed that recombinant human FGF8 was unable to stimulate nephron progenitor marker expression (including Cited1) and progenitor survival in nephrogenic zone cultures (whereas other FGF ligands did) (Brown et al., 2011). It is possible that Fgf8 is the ligand for Fgfr like-1 (Fgfrl1), an Fgf receptor that has a small intracellular domain that lacks a tyrosine kinase domain, and which when deleted largely phenocopies the kidney phenotype of the Fgf8 conditional knockout (Gerber et al., 2009). The fact that we did not observe a block in nephron development suggests that while Fgf receptor-Frs2α signaling is required for nephron progenitor renewal, it is dispensable for the mesenchyme to epithelial transition required for later stages of nephron formation.

Among the FGF ligands that drove nephron progenitor survival in the aforementioned nephrogenic zone cultures (FGF1, 2, 9 and 20) (Brown et al., 2011), Fgf2 is expressed by ureteric tips and was previously shown to sustain metanephric mesenchyme survival in rodent and Xenopus explants, alone or in combination with other growth factors (Perantoni et al., 1995; Barasch et al., 1997, 1999; Brennan et al., 1999; Plisov et al., 2001). Targeted deletion of *Fgf2* in mice, however, results in no kidney defects (Zhou et al., 1998), making it unlikely to be the (sole) endogenous ligand for Fgfr1 or Fgfr2. Also, *Fgf1* null mice have no apparent renal defects (alone or in combination with Fgf2) (Miller et al., 2000). In contrast, a recent publication revealed that global loss of *Fgf9* and/or *Fgf20* led to nephron progenitor apoptosis, loss of nephron progenitor stemness, and subsequent renal dysplasia that largely phenocopies our *Six2cre* mutant mice (Barak et al., 2012). Thus, Fgf9 and/or Fgf20 are likely endogenous ligands for Fgfr1 and/or Fgfr2 in the nephron progenitor compartment.

While Fgf9 and/or Fgf20 are likely the endogenous ligands for Fgfr1 and/or Fgfr2 in nephron progenitors, there are some apparent phenotypic differences between the ligand knockouts and the Fgfr/Frs2α knockouts in this study (Barak et al., 2012). First, Barak et al. did not describe cyst formation in their allelic series of Fgf9 and Fgf20 mutants; however, closer inspection of E16.5 and E18.5 mutant images (Figs. 1 and 2) reveal what appears to be a glomerular cyst and dilated LTL-positive tubules (Barak et al., 2012). Due to viability issues from lung maldevelopment, mutant Fgf9/20 mutant mice were not aged beyond E18.5; thus it is not possible to confirm that postnatal Fgf9/20 mutant mice would have developed marked numbers of cysts as in the postnatal Fgfr mutants, although it would seem likely. Second, Fgf9/20 mutants appeared to develop ectopic renal vesicles, which were not appreciated in the Fgfr mutants (Barak et al., 2012). Indeed, 3D reconstructions and *Wnt4*

section in situ hybridization in the Fgfr/ Frs2α allelic series failed to convincingly reveal ectopic renal vesicles in the receptor/Frs2α mutants (not shown). One possibility is that Fgf9 and/or Fgf20 are binding to and activating receptors in the renal stromal compartment and/or the ureteric epithelium in addition to the nephrogenic mesenchyme; thus, the loss of the ligands could lead to defects, such as ectopic vesicles, which are not seen in Six2cre Fgfr/ Frs2α mutants.

The $Fgfr1^{NP-/-}Fgfr2^{LR/LR}$ and $Fgfr1^{MM-/-}Fgfr2^{LR/LR}$ lines used in this and a previously published study (Sims-Lucas et al., 2012) reveal temporal and/or spatial windows of Fgfr activity in the metanephric mesenchyme lineage due to the different expression profiles of the *Cre* lines. $Fgfr1^{MM-/-}Fgfr2^{LR/LR}$ mice have both non-autonomous ureteric defects (morphogenesis and tubular dilatation/cysts) as well as autonomous defects (loss of nephron progenitors and tubular dilatation/cysts). In contrast, $Fgfr1^{NP-/-}Fgfr2^{LR/LR}$ mice have only autonomous defects (loss of nephron progenitors and nephron-derived cysts). One possible explanation for these differences lies in the timing of *Cre* expression in the two lines. The transgenic *Pax3*cre line deletes in early kidney mesenchyme (between E9.5 and 10.5) while the transgenic *Six2cre* line deletes slightly later in nephron progenitors (Li et al., 2000; Kobayashi et al., 2008). Another possible explanation is the difference in spatial expression of the two cre lines; the *Pax3cre* line drives gene deletion in both renal stromal and nephrogenic mesenchyme, whereas the *Six2cre* only targets the nephrogenic lineage. Interestingly, utilizing a *Foxd1cre* line (that deletes in the renal stromal lineage) to make "FFLR" mice resulted in no apparent ureteric or MM defects (unpublished observations). This does not exclude the possibility that Fgfrs in the nephrogenic and stromal lineages act cooperatively to regulate ureteric morphogenesis. Taken together, this is the first study revealing different temporal and/or spatial requirements for Fgfr signaling in the developing kidney mesenchyme.

The $Fgfr1/2^{NP-/-}$, $Fgfr1^{NP-/-}Fgfr2^{LR/LR}$, and $Frs2a^{NP-/-}$ allelic series also reveals additional insights into the relative roles of Frs2α-dependent signaling downstream of Fgfrs in the developing kidney. A previous study from our group showed that while both Fgfr2 and Frs2α are critical for ureteric branching morphogenesis, the two genes act independently in the epithelial ureteric lineage (Sims-Lucas et al., 2011b). In contrast, our current data strongly suggests that Frs2α is the main adapter protein for Fgfr signaling in the mesenchymal nephron progenitor lineage. First, the three *Six2cre* mutant mouse lines largely phenocopy one another. Second, among the non-Fgfr receptor tyrosine kinases (RTKs) that are known to utilize Frs2α′A′A i.e., Ret, neurotrophin receptors (Trks), and anaplastic lymphoma kinase (Alk), only Alk appears to be weakly expressed in nephron progenitors (GUDMAP Database: http://www.gudmap.org/); furthermore, *Alk*−/− mice have no overt kidney defects (Duyster et al., 2001). Other RTK mutants that result in kidney defects (i.e., Ret and TrkB) are not expressed in nephron progenitors and do not phenocopy our *Six2-EGFPcre* mutants (Schuchardt et al., 1994; Garcia-Suarez et al., 2006).

While all of the *Six2-EGFPcre*-driven mutants displayed similar defects (nephron progenitor loss, renal cystic hypodysplasia, etc.), the defects started earlier or were more severe in $Fgfr1/2^{NP-/-}$ mice compared to $Fgfr1^{NP-/-}Fgfr2^{LR/LR}$ mice, which in turn had more severe defects than $Frs2a^{NP-/-}$ mice. The most likely explanation is that other Fgf receptor

signaling adapters (e.g. PLC or Crk2) have minor roles in transmitting Fgf receptor signaling in nephron progenitors. Point mutations in docking sites on other receptor tyrosine kinases (RTKs), such as platelet derived growth factor receptor alpha, have shown additive effects of adapter signaling (Klinghoffer et al., 2002). Taken together, while Fgfr signaling appears to be independent of Frs2α in the ureteric epithelium, Fgfr signaling is most likely predominantly mediated by Frs2α in the mesenchymal nephron progenitors.

In investigating the mechanisms driving the nephron progenitor defects in the *Six2cre* mutants, we focused on candidate molecules/pathways known to regulate nephron progenitors. Among these, Bmp7, Wnt9b, p53, and Egf expression appeared to be unaltered in mutant nephron progenitors versus controls. The statistical decreases in Tgfα expression are unlikely to have significant biological relevance alone, although we cannot rule out the possibility that there is an additive effect if combined with alterations in expression of other genes that regulate progenitor survival. However, we detected evidence of increased Notch signaling in mutant nephron progenitors. Previous publications have shown that constitutive expression of either Notch1 or Notch2 in nephron progenitors (Cheng et al., 2007; Fujimura et al., 2010) leads to renal hypodysplasia, depletion of Six2 producing cells, and in the case of the *Notch2* mutants, the presence of renal cysts (Fujimura et al., 2010), similar to the findings in our mutant mice. In other systems, Fgf signaling has been shown to have antagonistic effects on Notch signaling (Small et al., 2003). Thus, we hypothesize that Fgfr/Frs2α signaling dampens Notch signaling in nephron progenitors to maintain the proper balance between progenitor survival versus differentiation.

In summary, we have demonstrated that Fgfr/Frs2α signaling controls the nephron progenitor population during renal development. As the kidney forms, Fgfr signaling through the Frs2α adapter protein regulates the number of Cited1 and Six2 expressing nephron progenitor cells, and also prevents progenitor cell apoptosis and the formation of mesenchymal cysts. This signaling axis is not required for nephron differentiation, but is needed for regulation of Notch signaling in the progenitor cell compartment. These results delineate a spatial and temporal requirement for Fgfr signaling during renal development and establish a cell autonomous role for signaling through Frs2α in the nephron progenitor compartment.

Supplementary Material

Refer to Web version on PubMed Central for supplementary material.

Acknowledgments

The authors thank Drs. Janet Rossant for the use of the floxed *Fgfr1* mouse line, Dr. Ornitz for the floxed *Fgfr2* mice, Dr. Eswarakumar for $Fgfr2^{LR}$ mice, Dr. Epstein for *Pax3cre mice* and Dr. Wang for floxed *Frs2α* mice. This study was supported by the National Institute of Diabetes and Digestive and Kidney Diseases Grants R01-DK095748 (CMB) and DK087794-04 (Jordan Kreidberg).

References

Arman E, Haffner-Krausz R, Chen Y, Heath JK, Lonai P. Targeted disruption of fibroblast growth factor (FGF) receptor 2 suggests a role for FGF signaling in pregastrulation mammalian development. Proc Natl Acad Sci USA. 1998; 95(9):5082–5087. [PubMed: 9560232]

Barak H, Huh SH, Chen S, Jeanpierre C, Martinovic J, Parisot M, Bole-Feysot C, Nitschke P, Salomon R, Antignac C, et al. FGF9 and FGF20 maintain the stemness of nephron progenitors in mice and man. Dev Cell. 2012; 22(6):1191–1207. [PubMed: 22698282]

Barasch J, Qiao J, McWilliams G, Chen D, Oliver JA, Herzlinger D. Ureteric bud cells secrete multiple factors, including bFGF, which rescue renal progenitors from apoptosis. Am J Physiol. 1997; 273(5 Pt 2):F757–F767. [PubMed: 9374839]

Barasch J, Yang J, Ware CB, Taga T, Yoshida K, Erdjument-Bromage H, Tempst P, Parravicini E, Malach S, Aranoff T, et al. Mesenchymal to epithelial conversion in rat metanephros is induced by LIF. Cell. 1999; 99(4):377–386. [PubMed: 10571180]

Blank U, Brown A, Adams DC, Karolak MJ, Oxburgh L. BMP7 promotes proliferation of nephron progenitor cells via a JNK-dependent mechanism. Development. 2009; 136(21):3557–3566. [PubMed: 19793891]

Boyle S, Misfeldt A, Chandler KJ, Deal KK, Southard-Smith EM, Mortlock DP, Baldwin HS, de Caestecker M. Fate mapping using Cited1-CreERT2 mice demonstrates that the cap mesenchyme contains self-renewing progenitor cells and gives rise exclusively to nephronic epithelia. Dev Biol. 2008; 313(1):234–245. [PubMed: 18061157]

Brennan HC, Nijjar S, Jones EA. The specification and growth factor inducibility of the pronephric glomus in *Xenopus laevis*. Development. 1999; 126(24):5847–5856. [PubMed: 10572058]

Brown AC, Adams D, de Caestecker M, Yang X, Friesel R, Oxburgh L. FGF/EGF signaling regulates the renewal of early nephron progenitors during embryonic development. Development. 2011; 138(23):5099–5112. [PubMed: 22031548]

Celli G, LaRochelle WJ, Mackem S, Sharp R, Merlino G. Soluble dominant-negative receptor uncovers essential roles for fibroblast growth factors in multi-organ induction and patterning. Embo J. 1998; 17(6):1642–1655. [PubMed: 9501086]

Cheng HT, Kim M, Valerius MT, Surendran K, Schuster-Gossler K, Gossler A, McMahon AP, Kopan R. Notch2, but not Notch1, is required for proximal fate acquisition in the mammalian nephron. Development. 2007; 134(4):801–811. [PubMed: 17229764]

Colvin JS, Bohne BA, Harding GW, McEwen DG, Ornitz DM. Skeletal overgrowth and deafness in mice lacking fibroblast growth factor receptor 3. Nat Genet. 1996; 12(4):390–397. [PubMed: 8630492]

Deng CX, Wynshaw-Boris A, Shen MM, Daugherty C, Ornitz DM, Leder P. Murine FGFR-1 is required for early postimplantation growth and axial organization. Genes Dev. 1994; 8(24):3045–3057. [PubMed: 8001823]

Di Giovanni V, Alday A, Chi L, Mishina Y, Rosenblum ND. Alk3 controls nephron number and androgen production via lineage-specific effects in intermediate mesoderm. Development. 2011; 138(13):2717–2727. [PubMed: 21613322]

Duyster J, Bai RY, Morris SW. Translocations involving anaplastic lymphoma kinase (ALK). Oncogene. 2001; 20(40):5623–5637. [PubMed: 11607814]

Eswarakumar VP, Ozcan F, Lew ED, Bae JH, Tome F, Booth CJ, Adams DJ, Lax I, Schlessinger J. Attenuation of signaling pathways stimulated by pathologically activated FGF-receptor 2 mutants prevents craniosynostosis. Proc Natl Acad Sci USA. 2006; 103(49):18603–18608. [PubMed: 17132737]

Fujimura S, Jiang Q, Kobayashi C, Nishinakamura R. Notch2 activation in the embryonic kidney depletes nephron progenitors. J Am Soc Nephrol. 2010; 21(5):803–810. [PubMed: 20299358]

Garcia-Suarez O, Gonzalez-Martinez T, Germana A, Monjil DF, Torrecilla JR, Laura R, Silos-Santiago I, Guate JL, Vega JA. Expression of TrkB in the murine kidney. Microsc Res Tech. 2006; 69(12):1014–1020. [PubMed: 17013912]

Gerber SD, Steinberg F, Beyeler M, Villiger PM, Trueb B. The murine Fgfrl1 receptor is essential for the development of the metanephric kidney. Dev Biol. 2009; 335(1):106–119. [PubMed: 19715689]

Gotoh N, Manova K, Tanaka S, Murohashi M, Hadari Y, Lee A, Hamada Y, Hiroe T, Ito M, Kurihara T, et al. The docking protein FRS2alpha is an essential component of multiple fibroblast growth factor responses during early mouse development. Mol Cell Biol. 2005; 25(10):4105–4116. [PubMed: 15870281]

Grieshammer U, Cebrian C, Ilagan R, Meyers E, Herzlinger D, Martin GR. FGF8 is required for cell survival at distinct stages of nephrogenesis and for regulation of gene expression in nascent nephrons. Development. 2005; 132(17):3847–3857. [PubMed: 16049112]

Hains D, Sims-Lucas S, Kish K, Saha M, McHugh K, Bates CM. Role of fibroblast growth factor receptor 2 in kidney mesenchyme. Pediatr Res. 2008; 64(6):592–598. [PubMed: 18670373]

Hains DS, Sims-Lucas S, Carpenter A, Saha M, Murawski I, Kish K, Gupta I, McHugh K, Bates CM. High incidence of vesicoureteral reflux in mice with Fgfr2 deletion in kidney mesenchyma. J Urol. 2010; 183(5):2077–2084. [PubMed: 20303521]

Hebert JM, Lin M, Partanen J, Rossant J, McConnell SK. FGF signaling through FGFR1 is required for olfactory bulb morphogenesis. Development. 2003; 130(6):1101–1111. [PubMed: 12571102]

Karner CM, Das A, Ma Z, Self M, Chen C, Lum L, Oliver G, Carroll TJ. Canonical Wnt9b signaling balances progenitor cell expansion and differentiation during kidney development. Development. 2011; 138(7):1247–1257. [PubMed: 21350016]

Klinghoffer RA, Hamilton TG, Hoch R, Soriano P. An allelic series at the PDGFalphaR locus indicates unequal contributions of distinct signaling pathways during development. Dev Cell. 2002; 2(1):103–113. [PubMed: 11782318]

Kobayashi A, Valerius MT, Mugford JW, Carroll TJ, Self M, Oliver G, McMahon AP. Six2 defines and regulates a multipotent self-renewing nephron progenitor population throughout mammalian kidney development. Cell Stem Cell. 2008; 3(2):169–181. [PubMed: 18682239]

Li J, Chen F, Epstein JA. Neural crest expression of Cre recombinase directed by the proximal Pax3 promoter in transgenic mice. Genesis. 2000; 26(2):162–164. [PubMed: 10686619]

Lin Y, Zhang J, Zhang Y, Wang F. Generation of an Frs2alpha conditional null allele. Genesis. 2007; 45(9):554–559. [PubMed: 17868091]

Little MH, McMahon AP. Mammalian kidney development: principles, progress, and projections. Cold Spring Harb Perspect Biol. 2012; 4:5.

Miller DL, Ortega S, Bashayan O, Basch R, Basilico C. Compensation by fibroblast growth factor 1 (FGF1) does not account for the mild phenotypic defects observed in FGF2 null mice. Mol Cell Biol. 2000; 20(6):2260–2268. [PubMed: 10688672]

Mugford JW, Yu J, Kobayashi A, McMahon AP. High-resolution gene expression analysis of the developing mouse kidney defines novel cellular compartments within the nephron progenitor population. Dev Biol. 2009; 333(2):312–323. [PubMed: 19591821]

Ong SH, Guy GR, Hadari YR, Laks S, Gotoh N, Schlessinger J, Lax I. FRS2 proteins recruit intracellular signaling pathways by binding to diverse targets on fibroblast growth factor and nerve growth factor receptors. Mol Cell Biol. 2000; 20(3):979–989. [PubMed: 10629055]

Ornitz DM, Marie PJ. FGF signaling pathways in endochondral and intramembranous bone development and human genetic disease. Genes Dev. 2002; 16(12):1446–1465. [PubMed: 12080084]

Perantoni AO, Dove LF, Karavanova I. Basic fibroblast growth factor can mediate the early inductive events in renal development. Proc Natl Acad Sci USA. 1995; 92(10):4696–4700. [PubMed: 7753867]

Perantoni AO, Timofeeva O, Naillat F, Richman C, Pajni-Underwood S, Wilson C, Vainio S, Dove LF, Lewandoski M. Inactivation of FGF8 in early mesoderm reveals an essential role in kidney development. Development. 2005; 132(17):3859–3871. [PubMed: 16049111]

Plisov SY, Yoshino K, Dove LF, Higinbotham KG, Rubin JS, Perantoni AO. TGF beta 2, LIF and FGF2 cooperate to induce nephrogenesis. Development. 2001; 128(7):1045–1057. [PubMed: 11245570]

Poladia DP, Kish K, Kutay B, Hains D, Kegg H, Zhao H, Bates CM. Role of fibroblast growth factor receptors 1 and 2 in the metanephric mesenchyme. Dev Biol. 2006; 291(2):325–339. [PubMed: 16442091]

Powers CJ, McLeskey SW, Wellstein A. Fibroblast growth factors, their receptors and signaling. EndocrRelat Cancer. 2000; 7(3):165–197.

Saifudeen Z, Liu J, Dipp S, Yao X, Li Y, McLaughlin N, Aboudehen K, El-Dahr SS. A p53–Pax2 pathway in kidney development: implications for nephrogenesis. PLoS One. 2012; 7(9):e44869. [PubMed: 22984579]

Schuchardt A, D'Agati V, Larsson-Blomberg L, Costantini F, Pachnis V. Defects in the kidney and enteric nervous system of mice lacking the tyrosine kinase receptor Ret [see comments]. Nature. 1994; 367(6461):380–383. [PubMed: 8114940]

Sims-Lucas S, Argyropoulos C, Kish K, McHugh K, Bertram JF, Quigley R, Bates CM. Three-dimensional imaging reveals ureteric and mesenchymal defects in Fgfr2-mutant kidneys. J Am Soc Nephrol. 2009a; 20(12):2525–2533. [PubMed: 19833900]

Sims-Lucas S, Cullen-McEwen L, Eswarakumar VP, Hains D, Kish K, Becknell B, Zhang J, Bertram JF, Wang F, Bates CM. Deletion of Frs2alpha from the ureteric epithelium causes renal hypoplasia. Am J Physiol Renal Physiol. 2009b; 297(5):F1208–F1219. [PubMed: 19741018]

Sims-Lucas S, Cusack B, Baust J, Eswarakumar VP, Masatoshi H, Takeuchi A, Bates CM. Fgfr1 and the IIIc isoform of Fgfr2 play critical roles in the metanephric mesenchyme mediating early inductive events in kidney development. Dev Dyn. 2011a; 240(1):240–249. [PubMed: 21128305]

Sims-Lucas S, Cusack B, Eswarakumar VP, Zhang J, Wang F, Bates CM. Independent roles of Fgfr2 and Frs2α in ureteric epithelium. Development. 2011b; 138(7):1275–1280. [PubMed: 21350013]

Sims-Lucas S, Di Giovanni V, Schaefer C, Cusack B, Eswarakumar VP, Bates CM. Ureteric morphogenesis requires Fgfr1 and Fgfr2/Frs2alpha signaling in the metanephric mesenchyme. J Am Soc Nephrol. 2012; 23(4):607–617. [PubMed: 22282599]

Small D, Kovalenko D, Soldi R, Mandinova A, Kolev V, Trifonova R, Bagala C, Kacer D, Battelli C, Liaw L, et al. Notch activation suppresses fibroblast growth factor-dependent cellular transformation. J Biol Chem. 2003; 278(18):16405–16413. [PubMed: 12598523]

Walker KA, Sims-Lucas S, Di Giovanni VE, Schaefer C, Sunseri WM, Novitskaya T, de Caestecker MP, Chen F, Bates CM. Deletion of fibroblast growth factor receptor 2 from the peri-Wolffian duct stroma leads to ureteric induction abnormalities and vesicoureteral reflux. PLoS One. 2013; 18(2):e56062. [PubMed: 23409123]

Weinstein M, Xu X, Ohyama K, Deng CX. FGFR-3 and FGFR-4 function cooperatively to direct alveogenesis in the murine lung. Development. 1998; 125(18):3615–3623. [PubMed: 9716527]

Xu X, Weinstein M, Li C, Naski M, Cohen RI, Ornitz DM, Leder P, Deng C. Fibroblast growth factor receptor 2 (FGFR2)-mediated reciprocal regulation loop between FGF8 and FGF10 is essential for limb induction. Development. 1998; 125(4):753–765. [PubMed: 9435295]

Yamaguchi TP, Harpal K, Henkemeyer M, Rossant J. fgfr-1 is required for embryonic growth and mesodermal patterning during mouse gastrulation. Genes Dev. 1994; 8(24):3032–3044. [PubMed: 8001822]

Zhao H, Kegg H, Grady S, Truong HT, Robinson ML, Baum M, Bates CM. Role of fibroblast growth factor receptors 1 and 2 in the ureteric bud. Dev Biol. 2004; 276(2):403–415. [PubMed: 15581874]

Zhou M, Sutliff RL, Paul RJ, Lorenz JN, Hoying JB, Haudenschild CC, Yin M, Coffin JD, Kong L, Kranias EG, et al. Fibroblast growth factor 2 control of vascular tone. Nat Med. 1998; 4(2):201–207. [PubMed: 9461194]

Appendix A. Supporting information

Supplementary data associated with this article can be found in the online version at http://dx.doi.org/10.1016/j.ydbio.2015.01.018.

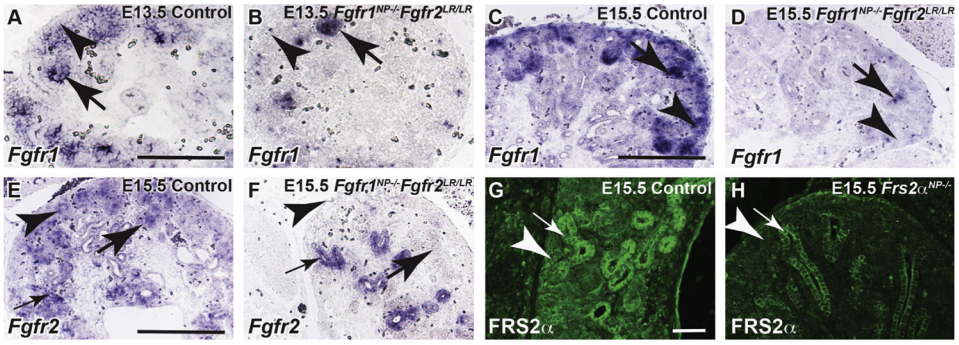

Fig. 1.

Efficiency of Six2-EGFPcre mediated *Fgfr* or Frs2α deletion. (A) In E13.5 control kidneys, *Fgfr1* mRNA is robustly expressed in the nephron progenitors (arrowheads) and developing nephron structures (arrow). (B) In E13.5 *Six2-EGFPcreFgfr1*$^{flox/flox}$*Fgfr2*$^{LR/LR}$ (*Fgfr1*$^{NP-/-}$*Fgfr2*$^{LR/LR}$) kidneys, nephron progenitors are devoid of *Fgfr1* mRNA (arrowhead), although rare nephron structures express *Fgfr1* mRNA (arrow), likely from early nephron progenitors that escaped cre mediated deletion. (C) In E15.5 control kidneys, *Fgfr1* mRNA is also expressed strongly in nephron progenitors (arrowhead) and developing nephron structures (arrow) (D) In E15.5 *Fgfr1*$^{NP-/-}$*Fgfr2*$^{LR/LR}$ kidneys, no nephron progenitors (arrowheads) and a very few nephron structures (arrow) express *Fgfr1* mRNA. (E) In E15.5 control kidneys, *Fgfr2* mRNA is observed in the nephron progenitors (arrowhead), developing nephron structures (arrow) and ureteric bud stalks (small arrow). (F) In E15.5 *Six2-EGFPcreFgfr1*$^{flox/flox}$*Fgfr2*$^{flox/flox}$ (*Fgfr1/2*$^{NP-/-}$) kidneys, *Fgfr2* expression is maintained in the ureteric bud stalks (small arrow) but absent from the nephron progenitors (arrowhead) and developing nephron structures (arrow). (G) In an E15.5 control kidney, Frs2α immunostaining (green) is observed in nephron progenitors (arrowhead), and the ureteric epithelium (small arrow). (H) In E15.5 *Six2-EGFPcreFrs2′A*$^{flox/flox}$ (*Frs2a*$^{NP-/-}$ kidneys), Frs2α′*A* staining is maintained in the ureteric epithelium (small arrow), but absent from nephron progenitors (arrowhead). A–F: scale bars=0.25 mm. G–H: scale bar=0.050 mm.

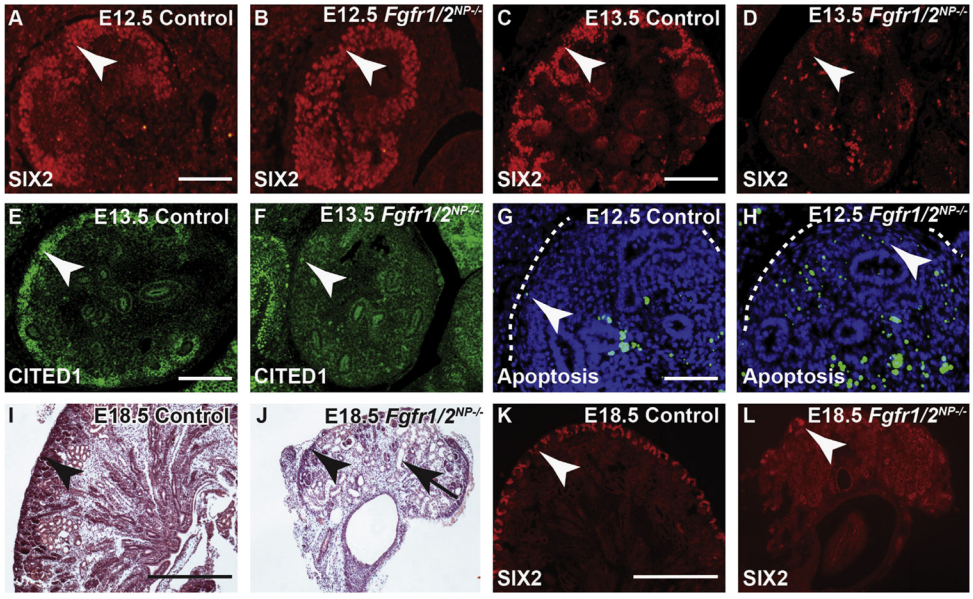

Fig. 2.

Fgfr1/2$^{NP-/-}$ mice have an early loss of nephron progenitors. (A, B) Six2 immunostaining appears similar in E12.5 control (A) and *Fgfr1/2*$^{NP-/-}$ (B) nephron progenitors (arrowheads). (C, D) Six2 immunostaining remains robust in E13.5 control (C) but markedly reduced in E13.5 *Fgfr1/2*$^{NP-/-}$ (D) nephron progenitors (arrowheads). (E, F) Cited1 immunostaining is present in E13.5 control nephron progenitors (E) and absent in E13.5 *Fgfr1/2*$^{NP-/-}$ (F) nephron progenitors (arrowheads). (G, H) TUNEL staining at E12.5 reveals a few apoptotic cells in control cap mesenchyme (G), but significantly more apoptotic cells in *Fgfr1/2*$^{NP-/-}$ (H) cap mesenchyme (arrowheads). Kidneys are outlined by dotted line. (I, J) H&E staining at E18.5 demonstrates a well-organized nephrogenic zone (arrowhead) in the control section (I), while the *Fgfr1/2*$^{NP-/-}$ mutant (J) has a sparse nephrogenic zone (arrowhead) and dilated tubules (arrow). (K, L) Six2 staining (red, arrowheads) reveals that compared to control (K) the *Fgfr1/2*$^{NP-/-}$ mutant (L) has very few remaining nephron progenitors. A–H: scale bars=0.050 mm. I–L: scale bars=0.25 mm.

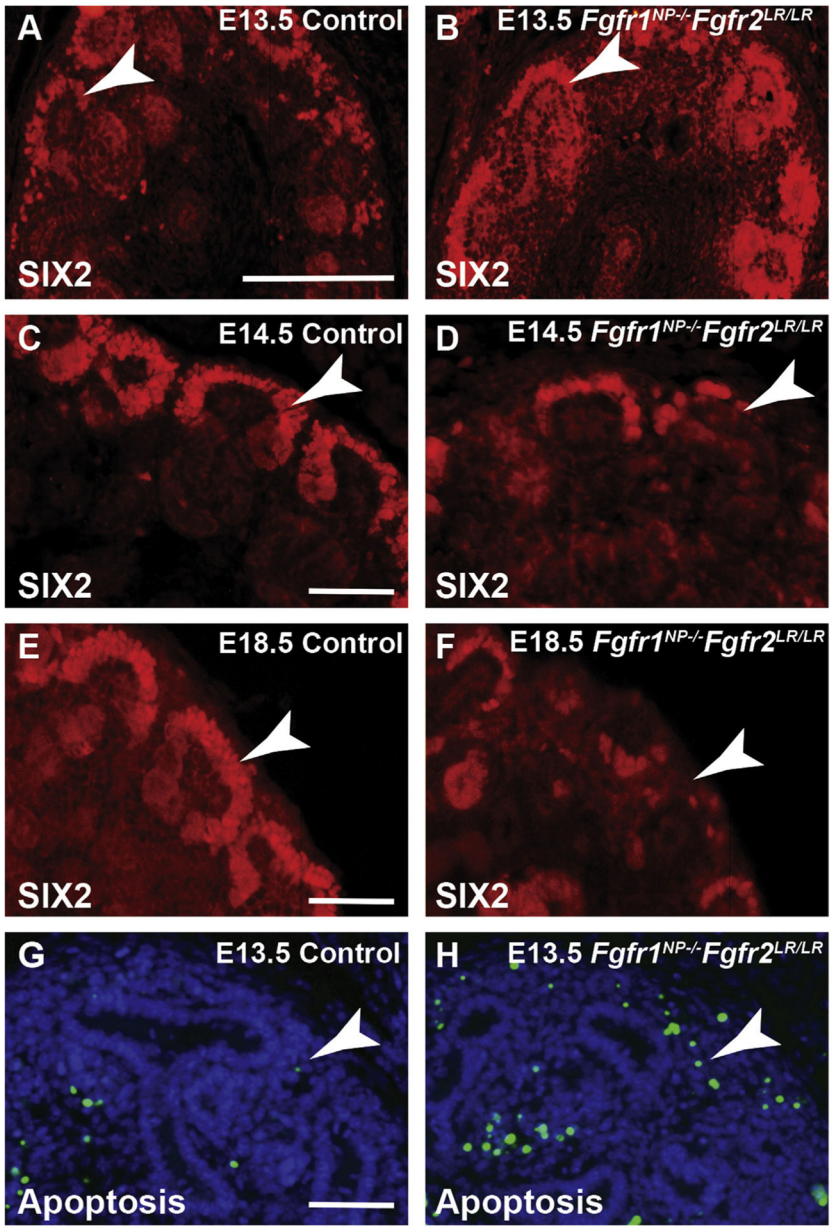

Fig. 3.

Fgfr1$^{NP-/-}$*Fgfr2*$^{LR/LR}$ embryos progressively lose nephron progenitors and have increased apoptosis. (A, B) At E13.5, the Six2 marked nephron progenitor cap mesenchyme population (red, arrowheads) appears similar in control (A) and *Fgfr1*$^{NP-/-}$*Fgfr2*$^{LR/LR}$ kidneys (B). (C, D) At E14.5, Six2 immunostaining (red, arrowheads) in control cap mesenchyme remains robust (C), but appears depleted in *Fgfr1*$^{NP-/-}$*Fgfr2*$^{LR/LR}$ kidneys (D), revealing diminished numbers of nephron progenitors. (E, F) At E18.5, Six2 immunostaining (red, arrowheads) reveals that compared to controls (E), *Fgfr1*$^{NP-/-}$*Fgfr2*$^{LR/LR}$ kidneys demonstrate severe losses in nephron progenitors. (G, H) E13.5 TUNEL staining (green, arrowheads) reveals a few apoptotic cells in the cap mesenchyme of controls (G), but statistically more apoptotic cells ($^{*}p<0.01$) in the cap

mesenchyme in *Fgfr1*$^{NP-/-}$*Fgfr2*$^{LR/LR}$ kidneys (H). A–B: scale bar=0.25 mm. C–H: scale bars=0.050 mm.

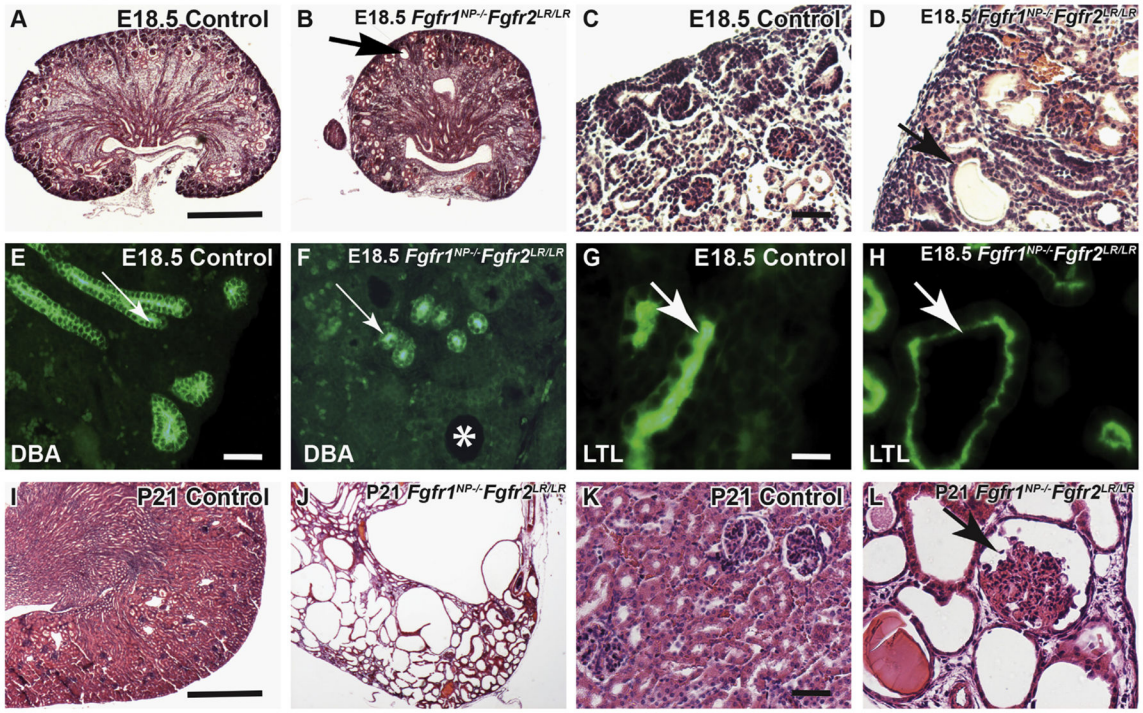

Fig. 4.

Older *Fgfr1*$^{NP-/-}$*Fgfr2*$^{LR/LR}$ kidneys develop cysts derived from mesenchyme. (A–D) E18.5H&E staining shows normal renal architecture in control kidneys (A, C), but dilated tubules (arrows) in *Fgfr1*$^{NP-/-}$*Fgfr2*$^{LR/LR}$ (B, D). (E, F) E18.5 DBA lectin staining (arrows) shows normal UB/collecting duct morphology in control kidney (E) and *Fgfr1*$^{NP-/-}$*Fgfr2*$^{LR/LR}$ kidney sections (F), although the latter has non-DBA labeled dilated tubules (asterisk). (G, H) E18.5 LTL lectin staining (arrows) identifies normal proximal tubules in control kidneys (G) and dilated proximal tubules in *Fgfr1*$^{NP-/-}$*Fgfr2*$^{LR/LR}$ (H). (I–L) P21 H&E staining reveals that compared to a control kidney (I, K), the *Fgfr1*$^{NP-/-}$*Fgfr2*$^{LR/LR}$ kidney (J, L) has cysts throughout the parenchyma, including in glomeruli (L, arrow). A,B, I,J: scale bar=0.75 mm. C–H, K,L: scale bar=0.050 mm.

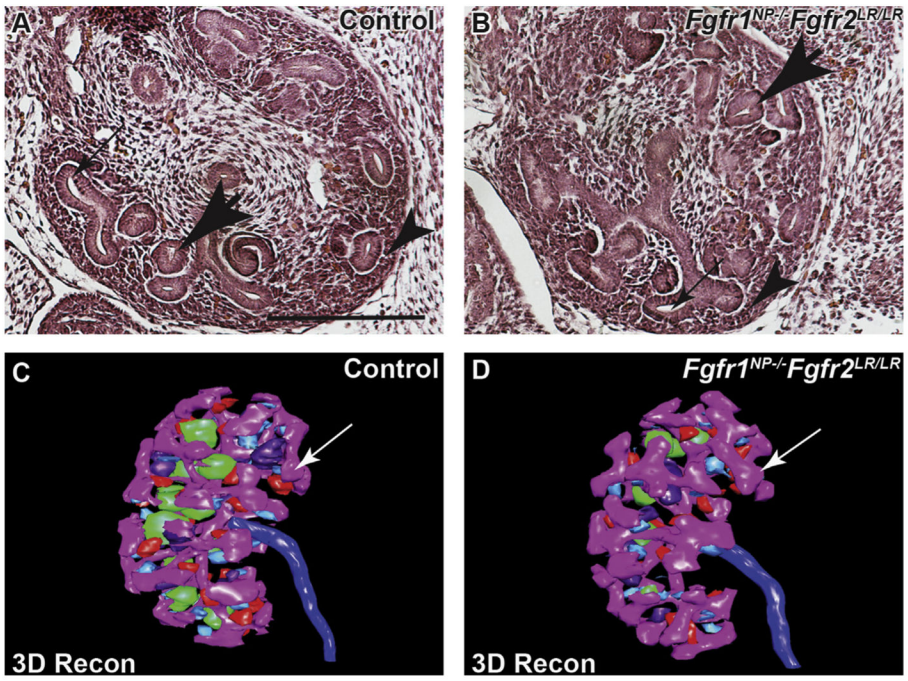

Fig. 5.

E13.5 *Fgfr1*$^{NP-/-}$*Fgfr2*$^{LR/LR}$ kidneys have normal ureteric morphogenesis. (A, B) E13.5H&E stain of a control kidney (A) and *Fgfr1*$^{NP-/-}$*Fgfr2*$^{LR/LR}$ kidney (B) shows normal UB tips (small arrows), nephron progenitors (arrowhead) and developing nephron structures (large arrows). Scale bar=0.25 mm. (C, D) 3D reconstructions of the E13.5 ureteric tree appear similar between controls (C) and *Fgfr1*$^{NP-/-}$*Fgfr2*$^{LR/LR}$ (D), including non-dilated ureteric tips (purple, arrows). In panels C and D: light blue shapes=renal vesicles, dark purple=comma shaped bodies, red=S-shaped bodies, green=immature glomeruli, and dark blue=ureter.

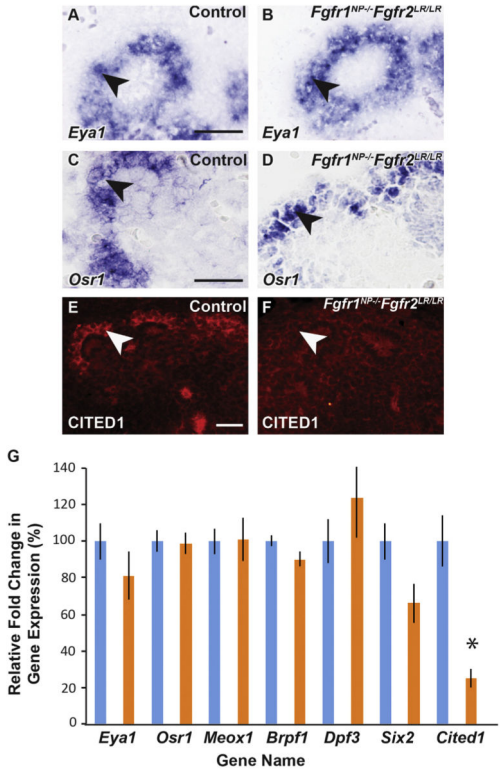

Fig. 6.

Profile of cap mesenchyme markers in E13.5 *Fgfr1*$^{NP-/-}$*Fgfr2*$^{LR/LR}$ nephron progenitors: (A–D) *Eya1* and *Osr1* expression by in situ hybridization (arrowheads) appears equivalent in controls (A, C) and *Fgfr1*$^{NP-/-}$*Fgfr2*$^{LR/LR}$ cap mesenchyme (B, D). (E, F) Cited1 expression by immunostaining (red, arrowheads) appears normal in control nephron progenitors (E) but virtually absent in *Fgfr1*$^{NP-/-}$*Fgfr2*$^{LR/LR}$ nephron progenitors (F). (G) Graph of qPCR data showing gene expression in control (blue) and *Fgfr1*$^{NP-/-}$*Fgfr2*$^{LR/LR}$ whole kidneys (orange) reveals a possible trend for decreased *Six2* mRNA expression (p=0.06) and statistically less *Cited1* mRNA ($^{*}p$<0.01) in the mutants, while the expression of other mesenchymal markers appears unchanged (all other genes p>0.05). A–D: scale bars=0.050 mm. E, F: scale bar=0.025 mm.

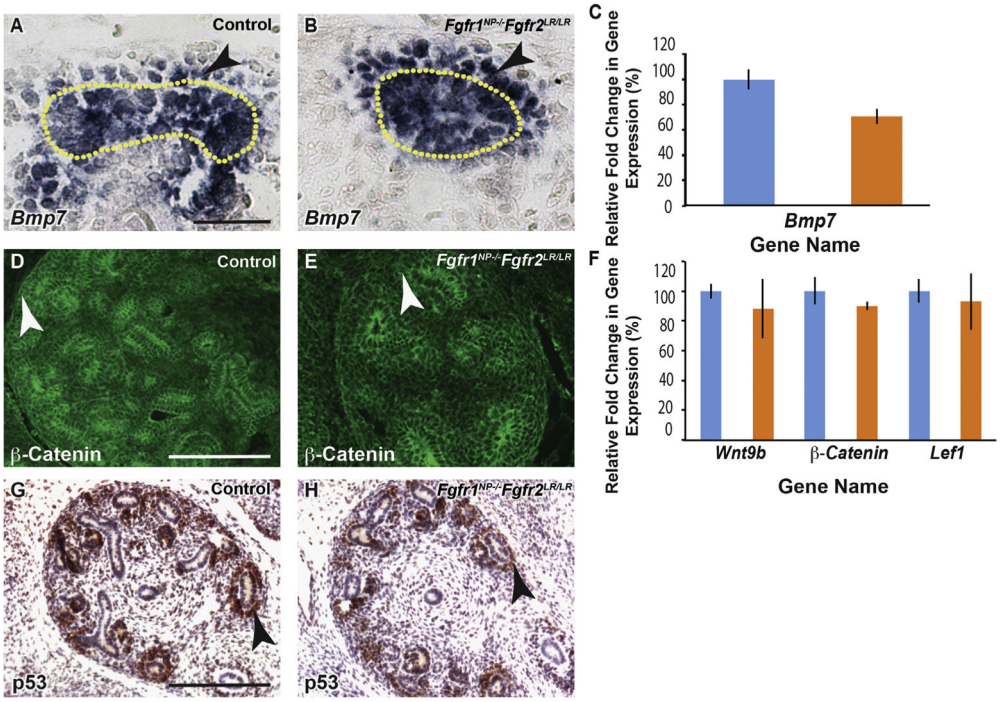

Fig. 7.

Bmp7, Wnt9b, and p53 appear similar in E13.5 *Fgfr1*$^{NP-/-}$*Fgfr2*$^{LR/LR}$ nephron progenitors. (A, B) In situ hybridization for *Bmp7* reveals similar expression levels in control (A) and *Fgfr1*$^{NP-/-}$*Fgfr2*$^{LR/LR}$ (B) nephron progenitors (arrowheads) that surround the *Bmp7*-positive ureteric tips (dotted lines). (C) Graph shows no change in *Bmp7* mRNA expression by qPCR in controls (blue bar) versus *Fgfr1*$^{NP-/-}$*Fgfr2*$^{LR/LR}$ kidneys (orange bar) (p=0.06). (D, E) Immunostaining for β-catenin is similar in control (D) and *Fgfr1*$^{NP-/-}$*Fgfr2*$^{LR/LR}$ (E) nephron progenitors (arrowheads). (F) Graph shows no change in relative mRNA expression of *Wnt9b* (p=0.52), *β-catenin* (p=0.35), or *Lef1* (p=0.66) by qPCR in *Fgfr1*$^{NP-/-}$*Fgfr2*$^{LR/LR}$ (orange bars) versus control kidneys (blue bars). (G, H) Immunostaining for p53 reveals similar expression levels in control (G) and *Fgfr1*$^{NP-/-}$ *Fgfr2*$^{LR/LR}$ (H) nephron progenitors (arrowheads). A, B: scale bar=0.050 mm. D, E, G, H: scale bars=0.25 mm.

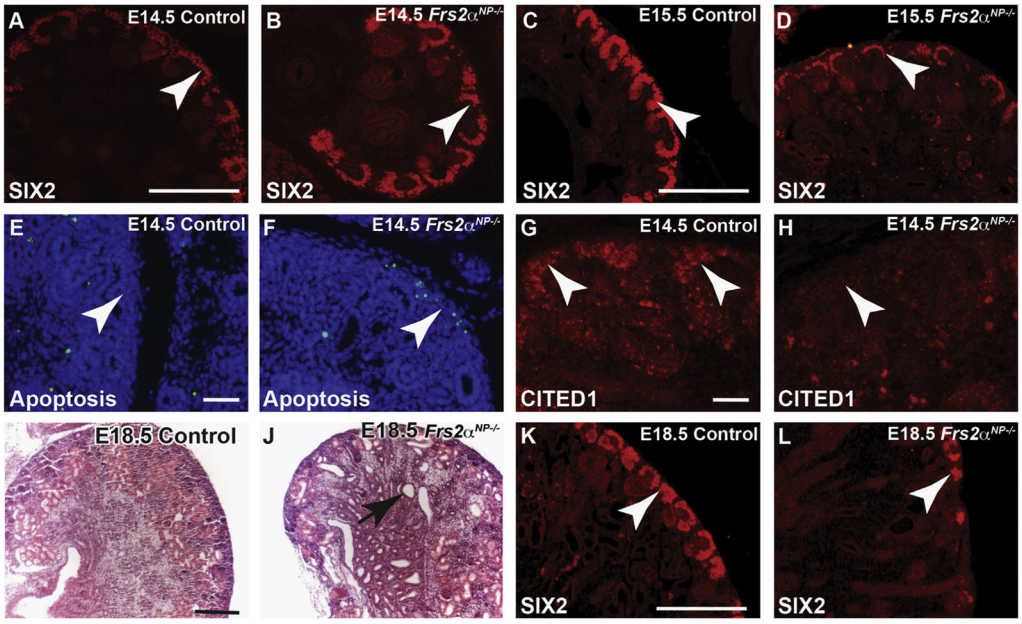

Fig. 8.

Frs2a$^{NP-/-}$ mice have a loss of nephron progenitors that is later than in *Fgfr1*$^{NP-/-}$*Fgfr2*$^{LR/LR}$ and *Fgfr1/2*$^{NP-/-}$ mice. (A, B) Six2 immunostaining (red, arrowheads) appears similar in E14.5 control (A) and *Frs2a*$^{NP-/-}$ (B) nephron progenitors. (C, D) Six2 immunostaining (red, arrowheads) remains robust in E15.5 control (C) but markedly reduced in E15.5 *Frs2a*$^{NP-/-}$ nephron progenitors (D). (E, F) TUNEL staining (green, arrowheads) at E14.5 reveals few apoptotic cells in control nephron progenitors (E), but many apoptotic cells in *Frs2a*$^{NP-/-}$ progenitors (F). (G, H) Cited1 immunostaining (red, arrowheads) is present in E14.5 control nephron progenitors (G) and absent in E14.5 *Frs2a*$^{NP-/-}$ nephron progenitors (H). (I, J) E18.5H&E section showing a normal control kidney (I) and a smaller *Frs2a*$^{NP-/-}$ kidney with dilated/cystic tubules (arrow). (K, L) Six2 staining reveals that in contrast to the control (K) the Six2 marked nephron progenitors (arrowheads) are severely depleted in E18.5 *Frs2a*$^{NP-/-}$ mutants (L). A–D, I–L: Scale bars=0.25 mm. E, F: Scale bars=0.050 mm. G, H: Scale bars=0.020 mm.

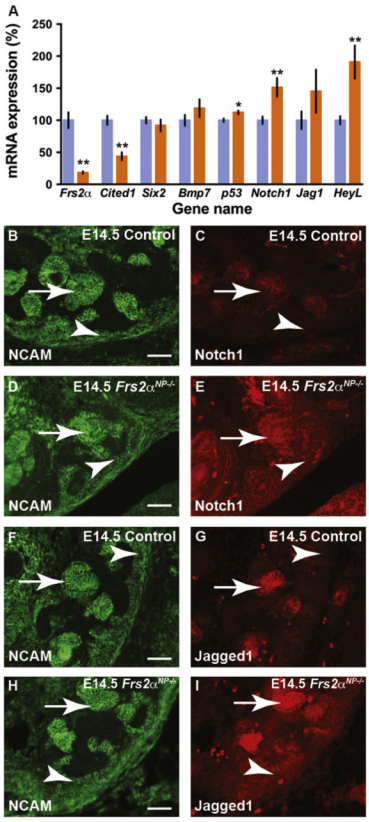

Fig. 9.

Frs2a$^{NP-/-}$ mice have increased Notch signaling in E14.5 nephron progenitors. (A) Graph of relative gene expression by qPCR in FAC-sorted E14.5 nephron progenitors demonstrates significantly decreased *Frs2α′A* and *Cited1′A* ***′A*<0.01′*A*, unaltered *Six2* and *Bmp7* (both $p>0.05$), marginally increased *p53* ($^{*}p<0.05$), trends for increased *Jagged1* ($p=0.1$), and significantly elevated *Notch1* and *HeyL* ($^{*}p<0.01$) in *Frs2a*$^{NP-/-}$ (orange bars) versus controls (blue bars). (B, C) Immunostaining for NCAM (B) and Notch 1 (C) in adjacent sections reveals limited Notch staining in nephron progenitors (arrowheads) but detectable expression in developing nephron structures (arrows) in controls. (D, E) Immunostaining for NCAM (D) and Notch1 (E) in *Frs2a*$^{NP-/-}$ kidneys reveals stronger NCAM stained nephron progenitors (arrowheads) and possibly in developing nephron structures (arrows). (F–I) Immunostaining for NCAM in controls (F) and *Frs2a*$^{NP-/-}$ (H) and Jagged1 in control (G) and *Frs2a*$^{NP-/-}$ (I) reveals increased Jagged 1 expression in mutant nephron progenitors (arrowheads) and possibly in developing nephron structures (arrows). B–: Scale bars=0.050 mm.